© The American Society of Gene & Cell Therapy

Restoration of Cone Vision in the CNGA3$^{-/-}$ Mouse Model of Congenital Complete Lack of Cone Photoreceptor Function

Stylianos Michalakis[1], Regine Mühlfriedel[2], Naoyuki Tanimoto[2], Vidhyasankar Krishnamoorthy[3], Susanne Koch[1], M Dominik Fischer[2], Elvir Becirovic[1], Lin Bai[1], Gesine Huber[2], Susanne C Beck[2], Edda Fahl[2], Hildegard Büning[4], François Paquet-Durand[5], Xiangang Zong[1], Tim Gollisch[3], Martin Biel[1] and Mathias W Seeliger[2]

[1]Center for Integrated Protein Science Munich (CIPSM), Department of Pharmacy–Center for Drug Research, Ludwig-Maximilians-Universität München, Munich, Germany; [2]Division of Ocular Neurodegeneration, Institute for Ophthalmic Research, Centre for Ophthalmology, Eberhard Karls-Universität, Tübingen, Germany; [3]Visual Coding Group, Max Planck Institute of Neurobiology, Martinsried, Germany; [4]Department I of Internal Medicine and Center for Molecular Medicine Cologne, University of Cologne, Cologne, Germany; [5]Division of Experimental Ophthalmology, Institute for Ophthalmic Research, Centre for Ophthalmology, Eberhard Karls-Universität, Tübingen, Germany

Congenital absence of cone photoreceptor function is associated with strongly impaired daylight vision and loss of color discrimination in human achromatopsia. Here, we introduce viral gene replacement therapy as a potential treatment for this disease in the CNGA3$^{-/-}$ mouse model. We show that such therapy can restore cone-specific visual processing in the central nervous system even if cone photoreceptors had been nonfunctional from birth. The restoration of cone vision was assessed at different stages along the visual pathway. Treated CNGA3$^{-/-}$ mice were able to generate cone photoreceptor responses and to transfer these signals to bipolar cells. In support, we found morphologically that treated cones expressed regular cyclic nucleotide-gated (CNG) channel complexes and opsins in outer segments, which previously they did not. Moreover, expression of CNGA3 normalized cyclic guanosine monophosphate (cGMP) levels in cones, delayed cone cell death and reduced the inflammatory response of Müller glia cells that is typical of retinal degenerations. Furthermore, ganglion cells from treated, but not from untreated, CNGA3$^{-/-}$ mice displayed cone-driven, light-evoked, spiking activity, indicating that signals generated in the outer retina are transmitted to the brain. Finally, we demonstrate that this newly acquired sensory information was translated into cone-mediated, vision-guided behavior.

Received 11 April 2010; accepted 15 June 2010; published online 13 July 2010. doi:10.1038/mt.2010.149

INTRODUCTION

The cone photoreceptor cyclic nucleotide-gated (CNG) channel stands at the end of the phototransduction process and translates light-dependent changes of cyclic guanosine monophosphate (cGMP) levels into electrical activity, which in turn controls release of neurotransmitters at the synapses to secondary neurons. The channel is a heterotetramer composed of two CNGA3 and CNGB3 subunits.[1] Mutations in the genes that encode either of the two types of subunits account together for ~75% of all cases of complete achromatopsia,[2] a hereditary, autosomal recessive disorder characterized by lack of cone photoreceptor function. In contrast to color blindness, in which changes in expression of opsin genes merely affect spectral sensitivity but not the physiology of photoreceptors,[3,4] the complete unresponsiveness of cones in achromatopsia has grave consequences for vision, particularly with respect to the densely cone-packed human fovea. In addition to the lack of color discrimination, achromats suffer from very poor visual acuity, pendular nystagmus, and photophobia.[5]

We have previously shown that genetic inactivation of CNGA3 in mice—in close agreement with the human phenotype—leads to selective loss of cone-mediated light responses[6] accompanied by morphological, structural, and molecular changes, and finally results in cone cell death.[7] These changes include a disorganization of membrane structure of cone outer segments, downregulation and mislocalization of cone opsins, and downregulation of additional outer segment proteins. Importantly, all of these changes become evident several days before completion of cone photoreceptor development (*i.e.*, before eye opening).[7] Cone degeneration is evident from the second postnatal week onward and proceeds significantly faster in ventral and nasal than in dorsal and temporal parts of the retina. Ventral cones are almost completely missing after the third postnatal month whereas residual dorsal cones are present even in aged knockout mice.[7]

Recently, the successful treatment of retinal degeneration using recombinant adeno-associated viral (rAAV) vectors has been demonstrated in animal models,[8,9] and has now led to

S.M. and R.M. contributed equally to this work. M.B. and M.W.S. contributed equally to this work.

Correspondence: *Martin Biel, Department Pharmazie–Pharmakologie für Naturwissenschaften, Ludwig-Maximilians-Universität München, Butenandtstr. 5-13, D-81377 München, Germany. E-mail: mbiel@cup.uni-muenchen.de or Mathias W Seeliger, Division of Ocular Neurodegeneration, Institute for Ophthalmic Research, Centre for Ophthalmology, Eberhard Karls-Universität, Schleichstr. 4/3, 72076 Tuebingen, Germany. E-mail: see@uni-tuebingen.de*

© The American Society of Gene & Cell Therapy

human clinical trials.[10–13] A positive effect of gene therapy on cone function at a retinal level has also been found in a hypomorph cone transducin mutant[14] (Gnat2^{cpfl3} mouse) with residual protein expression and cone electroretinogram (ERG) responses (~25% of normal at 4 weeks of age), and no obvious cone degeneration.[15]

We set out to design a curative treatment strategy using rAAV5 vectors with the mouse blue cone opsin promoter to restore cone function in the CNGA3$^{-/-}$ mouse model. Some of the challenges we had to face relate to the lack of basic knowledge about the behavior of the cone visual system in disease conditions. In particular, at the beginning of the project it was unclear whether (i) an outer segment ion channel can be functionally expressed in the nonfunctional, morphologically compromised, and degenerating CNGA3$^{-/-}$ cone photoreceptors, (ii) the massive deregulation of the cone-signaling cascade in CNGA3$^{-/-}$ mice can be functionally restored to recover light-triggered responsiveness, and (iii) the congenitally achromatic CNGA3$^{-/-}$ mice can use this new cone photoreceptor-specific information to produce vision-guided behavior.

In this study, we have addressed these major problems. We show that rAAV-mediated gene replacement therapy rescues functional defects resulting from the congenital absence of the CNGA3 channel. Furthermore, recordings of light-evoked ganglion cell activity under photopic conditions illustrate that cone signals in treated retinas are transmitted to the inner retina and then to downstream brain areas. In addition, we also demonstrate in a behavioral test that gene replacement bestows cone-mediated vision on CNGA3$^{-/-}$ mice.

RESULTS

Gene delivery was achieved by means of the rAAV system. Specifically, we designed rAAV vectors that drive expression of the mouse CNGA3 complementary DNA under control of a 0.5-kb fragment of the mouse blue opsin (S-opsin) promoter.[16] We packaged the viral vector particles with a Y719F-modified AAV5 capsid (AAV5-mBP-CNGA3) that results in higher resistance to proteasomal degradation.[17] We delivered 6–9 × 10^9 rAAV genomic particles into the subretinal space within the central to ventral part of the retina of 12- to 14-day-old CNGA3$^{-/-}$ mice and monitored the procedure immediately following the injections using scanning laser ophthalmoscopy[18] and optical coherence tomography.[19]

At 10 weeks post-treatment, clear signs of a functional restoration of cone photoreceptor function were found in Ganzfeld ERGs (**Figure 1**). No differences between the treated eyes, untreated eyes, or wild-type eyes were detectable at dim-light levels (**Figure 1a**, top row), demonstrating regular rod function. A prominent rescue effect on cones was found in the light-adapted (photopic) part of the protocol (**Figure 1a**, bottom), in which rods are non-responsive due to desensitization. Next, we used an additional stimulus protocol, the 6 Hz scotopic flicker ERG (**Figure 1b**), in which the increasing stimulus intensity leads to a transition from rod- to cone-dominated responses.[20] The difference between the untreated eyes (black traces), which reflect pure rod responses, and the treated eyes (red traces), clearly shows the functional benefit with growing intensity. The comparison with a rhodopsin knockout (rho$^{-/-}$) model[21] indicates the contribution of the cone

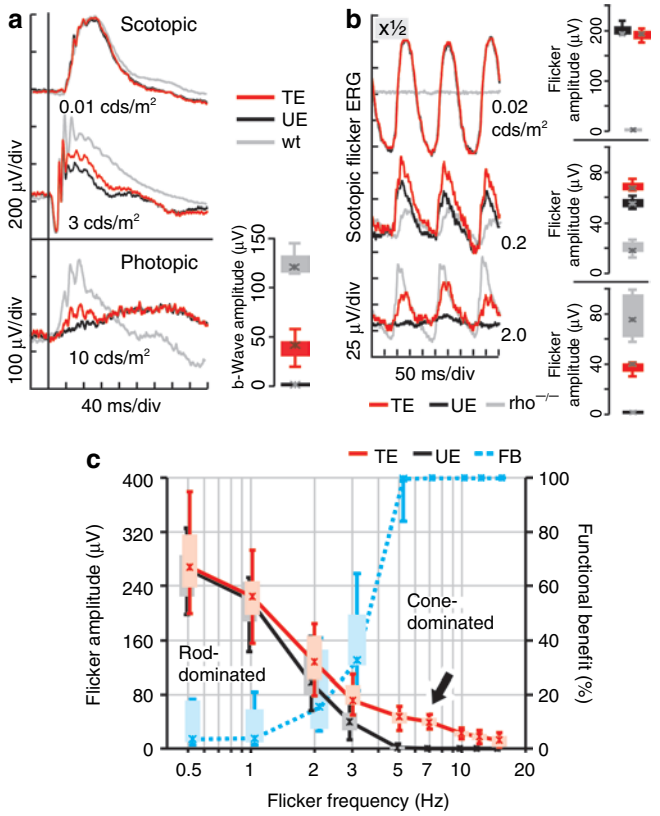

Figure 1 Restoration of cone-mediated electroretinogram (ERG) in treated CNGA3$^{-/-}$ mice. Traces are from representative animals, box plots summarize the group data. (**a**) Single flash ERG. Scotopic rod system response (top): No difference between the treated eye (TE), untreated eye (UE), and the wild-type (wt) eye. Mixed rod/cone system response (center): amplitude increase in the TE relative to the UE indicative for cone system function improvement. Photopic conditions (traces bottom left, corresponding box plot bottom right): substantial restoration of cone system function. (**b**) Scotopic 6 Hz flicker ERG intensity series. Left column: traces obtained at three selected stimulus intensities; right column: corresponding box plots. Top: no difference in the rod-specific response (1/2 size to facilitate comparison) between TE and UE, no cone system contribution (confirmed by rho$^{-/-}$). Center: responses to an intermediate stimulus. The waveform difference between TE and UE (red versus black trace) is due to the time lag of the cone response (grey trace) relative to the rod response (black trace). Bottom: responses to a cone-specific bright stimulus. The difference between TE and UE is clearly visible. (**c**) Functional benefit from treatment as a function of ERG flicker frequency (flash intensity 3 cds/m²). Red (TE) and black (UE) traces represent amplitude data, the blue trace represents the functional benefit (FB) in percent calculated as (TE – UE)/TE amplitudes. At low frequencies up to about 2–3 Hz, the responses are dominated by the rod system, and at about 5 Hz and above, by the cone system, where the benefit of restoring cone functionality is maximal.

system at each intensity level. At intermediate stimulus intensities (**Figure 1b**, center), the cone responses (gray traces), due to their lower light sensitivity, are slightly delayed relatively to the rod responses (black traces), leading to a slightly shifted appearance of the mixed response waveform in treated eyes. At high flash intensities, when rod function is almost absent, the treatment effect on cones again became particularly obvious (**Figure 1b**, bottom). Finally, we assessed the functional benefit with flashes of a given intensity but varying frequency (**Figure 1c**), a protocol that allows for a reliable separation of rod and cone system responses.[22] We

© The American Society of Gene & Cell Therapy

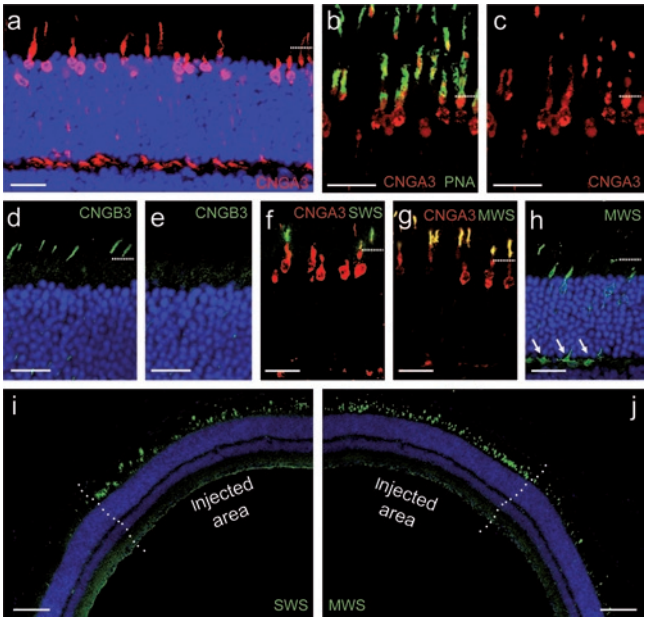

Figure 2 Establishment of cone cyclic nucleotide-gated (CNG) channel and restoration of opsin expression in treated CNGA3$^{-/-}$ cones. (**a–c**) Cone-specific expression of CNGA3 (red) in a treated area of a CNGA3$^{-/-}$ retina. (**b**,**c**) Co-labeling with the cone marker peanut agglutinin (PNA) indicates presence of rescued CNGA3 in cone outer segments (COS). (**b**) Merged image (PNA, green; CNGA3, red). (**c**) CNGA3 signal alone. (**d–j**) CNGA3 replacement restores expression and correct localization of visual cascade proteins. (**d**) Recovery of CNGB3 expression in COS in treated retina. (**e**) Absence of the CNGB3 subunit in untreated COS. Specific normalization of short wavelength opsin (**f**,**i**) and medium wavelength opsin (**g**,**j**) in COS of injected areas of the retina. (**h**) Representative image showing cone opsin (here medium wavelength) mislocalization in an age-matched untreated CNGA3$^{-/-}$ retina (arrows point to mislocalized opsin within the synapses). Bars = 20 µm in **a–h**; 100 µm in **i–j**. Horizontal bars in **a–d** and **f–h**) mark the outer-to-inner segment border. In **a**,**d–e**, and **h–j** nuclei are stained with Hoechst dye (blue).

found that the fraction of the ERG attributed to the restored cone system rises with flash frequency, and above about 5 Hz constitutes the entire response (arrow in **Figure 1c**). This indicates that our gene therapeutic treatment provides a substantial, cone-specific functional benefit to CNGA3$^{-/-}$ mice.

The ERG measurements suggested a substantial restoration of the severely impaired visual cascade in treated CNGA3$^{-/-}$ mice. To assess this in detail, eyes of treated mice were removed, fixed, cryosectioned, and processed for immunohistochemistry (**Figure 2**) upon completion of ERG measurements. In agreement with the ERG recordings, we found expression of CNGA3 in cone photoreceptors within the injected but not the untreated part of the retina. It turned out that a single subretinal injection (1–1.5 µl volume) covered ~30% of the total retinal area. The CNGA3 protein was specifically expressed in cones and localized throughout the cone photoreceptor (**Figure 2a**). Importantly, substantial amounts of protein (comparable to wild-type levels) were localized within cone outer segments (**Figure 2b,c**). The CNGA3 protein that was produced as a result of our therapy was able to restore cone outer segments expression and localization of CNGB3 (**Figure 2d,e**). This suggests the presence of regular heteromeric CNG channels in the outer segments.

We have previously shown that S cones are the first to degenerate in the CNGA3$^{-/-}$ retina and that virtually no S-opsin can be detected in 3-month-old knockout retina.[7] To evaluate the survival of S cones in the treated regions and to validate the cone subtype-specificity of mBP-driven expression we stained the retinas of treated eyes with cone opsin-specific antibodies (**Figure 2f–j**). S-opsin (short wavelength) labeling was detected in a subpopulation of CNGA3-positive cone outer segments in the treated part of the retina (**Figure 2f,i**), confirming successful rescue of S cones. Co-labeling for M-opsin (medium wavelength) and CNGA3 identified many M-opsin-positive treated cones (**Figure 2g,j**) suggesting that the mBP promoter drives cone-specific expression in both cone subtypes of the mouse. Importantly, gene replacement therapy reestablished normal expression and localization of cone opsins (**Figure 2f,g**) that were downregulated and mislocalized in untreated CNGA3$^{-/-}$ mice (**Figure 2h**).

Within the untreated part of the retina all surviving cones showed profound accumulation of cGMP (green in **Figure 3a–d**, detected using a cGMP-specific antibody[23]), which may result from continuous activation of the guanylyl cyclase by Ca^{2+}-free GCAP[24,25] in CNGA3$^{-/-}$ cones. This accumulation of cGMP is restricted to cones and begins several days before eye opening (**Figure 3c–e**). Expression of CNGA3 lowered cGMP to wild-type levels indicating that the Ca^{2+}-triggered feedback inhibition of the guanylyl cyclase is reestablished in treated cones (**Figure 3a,b**). Müller glial cells respond to retinal degeneration by upregulation of intermediate filament proteins (stress fibers, *e.g.*, glial fibrilary acid protein), which is typically observed in the untreated CNGA3$^{-/-}$ retina[7] (**Figure 3f**). Expression of CNGA3 markedly lowered the number of glial fibrilary acid protein–positive stress fibers (**Figure 3g**), suggesting that the treatment was able to reduce the degenerative process in the retina. In support of this, high numbers of cones are still present in the ventral retina of treated (**Figure 3h**) but not untreated (age-matched) CNGA3$^{-/-}$ mice (**Figure 3i**).

Having shown by electroretinography that treated cones acquired the ability to generate regular light-evoked signals and to activate respective bipolar cells, we next examined whether these signals are capable of exciting ganglion cells in a regular fashion. To this end, we performed multielectrode array recordings to measure the spiking activity of ganglion cells from isolated retinas of treated and untreated eyes of CNGA3$^{-/-}$ mice (**Figure 4a–d**). As expected for a retina limited to rod function only, ganglion cells from untreated CNGA3$^{-/-}$ mice responded well at low-light levels, but did not show any light-evoked activity under photopic conditions (**Figure 4b,d**). Much in contrast, many neurons in treated regions displayed strong light-evoked activity for both low- and high-light levels (**Figure 4a,c**). Specifically, 33 out of a total of 46 recorded ganglion cells from three retinas displayed clear light-evoked spiking activity at photopic light levels, indicating that transmission of cone signals to the inner retina was reestablished in the treated retinas.

Among these 33 ganglion cells with photopic responses, the response characteristics revealed ON-type cells, as well as OFF-type and ON–OFF-type cells. Most cells had the same response type at all light levels (12 ON cells, 11 OFF cells, 6 ON–OFF cells); four cells had ON–OFF characteristics at low-light intensity, but

© The American Society of Gene & Cell Therapy

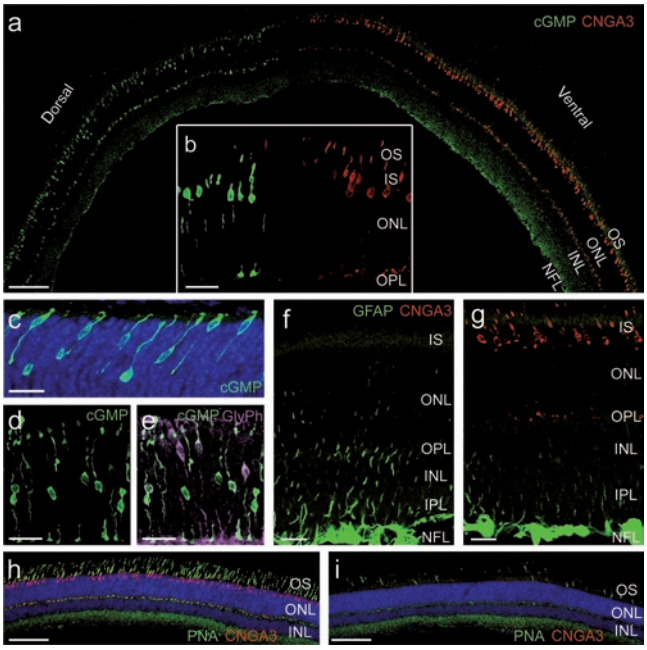

Figure 3 Establishment of a functional visual cascade and delay of degeneration in treated CNGA3$^{-/-}$ cones. (**a**) Compiled overview image of a treated CNGA3$^{-/-}$ retina stained for cGMP (green) and CNGA3 (red). Cone photoreceptors outside of the injected region (dorsal) contain high levels of cGMP. Expression of CNGA3 protein normalizes cGMP. (**b**) Higher magnification image of the treatment-border area from another treated CNGA3$^{-/-}$ retina stained for cGMP (green) and CNGA3 (red). (**c**) Cone-specific cGMP accumulation (green) in the CNGA3$^{-/-}$ retina at postnatal day 4 (8 days before eye opening). (**d**,**e**) All cGMP-positive (**d**, green) cells in a 12-day-old CNGA3$^{-/-}$ retina are positive for the cone marker (**e**) glycogen phosphorylase (GlyPh, magenta). (**f**) Untreated mice show marked elevation of GFAP-positive (green) stress fibers in inner retinal layers. (**g**) Treatment keeps GFAP stress fibers at low levels. Note that Müller cell end feet within the neurofilanent layer are GFAP-positive in treated and untreated mice. (**h**,**i**) The treatment preserves a high number of cones within the ventral retina. Retinal slices of age-matched treated and untreated CNGA3$^{-/-}$ mice were stained with the cone marker peanut agglutinin (PNA, green) and anti-CNGA3 (red). Bar = 100 µm in **a**,**h**, and **i**; 20 µm in **b**–**g**. In **c**,**h**, and **i**, nuclei are stained with Hoechst dye (blue). cGMP, cyclic guanosine monophosphate; GFAP, glial fibrilary acid protein; INL, inner nuclear layer; IPL, inner plexiform layer; IS, (photoreceptor) inner segments; NFL, neurofilament layer; ONL, outer nuclear layer; OPL, outer plexiform layer; OS, (photoreceptor) outer segments.

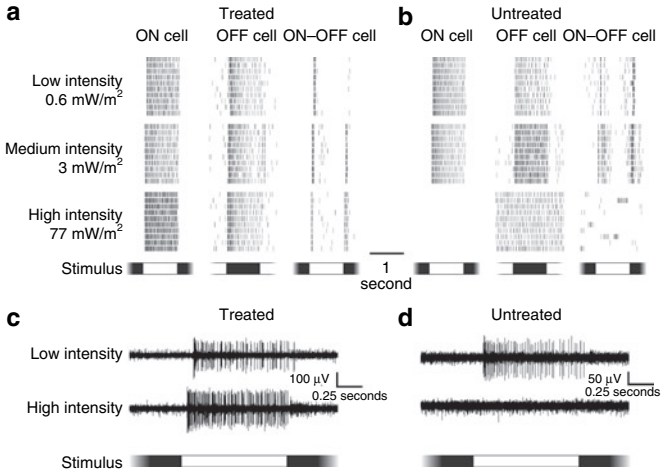

Figure 4 Gene replacement therapy restores responsiveness of ganglion cells to photopic stimuli in CNGA3$^{-/-}$ mice. (**a**,**b**) Spike trains of different types of ganglion cells from (**a**) treated and (**b**) untreated CNGA3$^{-/-}$ mice. Spikes were measured in response to periodic flashes of light at three different intensity levels (left). For each condition, responses to 10 successive presentations are shown. Stimulus phase is indicated at the bottom. The spike trains obtained from the treated mice show reliable response patterns for all applied light intensities. By contrast, ganglion cells from untreated retinas do not respond to light flashes at the highest light level, which corresponds to photopic conditions. Instead, some cells at this light level display spontaneous activity, which is not locked to the stimulus presentation. (**c**,**d**) Sample voltage traces recorded from the ON cells shown in **a** and **b**, respectively.

were classified as either ON-type or OFF-type at high-light level. These results indicate that all major response types of ganglion cells are restored by the treatment and that the basic cell-type specification is upheld.

Finally, we aimed at assessing whether the restoration of retinal cone-mediated signaling enabled treated CNGA3$^{-/-}$ mice to develop cone vision-guided behavior. We therefore designed a simple test for vision-guided behavior in mice that highly depends on cone-mediated vision under photopic light conditions (see Materials and Methods). The mice were trained in a cued water maze to associate a red cue with a stable visible platform (day one, see **Supplementary Video S1**). On day 2, the mice had to discriminate between two randomly arranged visible platforms (see **Supplementary Video S2**), a stable platform marked with a red cue (correct choice) and a platform that sank when a mouse climbed onto it marked with a green cue (incorrect choice). Wild-type mice were able to differentiate between the two platforms based on the visual cues and performed significantly above chance level (**Figure 5a**, 76.4 ± 4.3% correct choices, $N = 12$, one sample t-test, $P = 0.003$). This indicates that wild-type mice were able to differentiate between the two cues. Note that the mice may have used differences in the spectral identity, luminous intensity, or some combination of the two to discriminate between the two visual cues. The fact that cone-mediated vision is essential for stimulus discrimination, however, was confirmed by the fact that CNGA3$^{-/-}$ mice were not able to solve this task; their performance was not significantly different from the 50% chance level (**Figure 5a**, 55.6 ± 3.7% correct choices, $N = 12$, one sample t-test, $P = 0.328$). Treated CNGA3$^{-/-}$ mice, on the other hand, performed significantly better than untreated CNGA3$^{-/-}$ mice (**Figure 5a**, 73.8 ± 5.0% correct choices, $N = 7$, $P = 0.009$). Moreover, treated CNGA3$^{-/-}$ mice showed no significant difference to the wild-type control mice in this test ($P = 0.711$). This confirms that our gene replacement therapy is sufficient to restore cone-mediated visual behavior.

In addition, we tested CNGA3/CNGB1 double knockout mice that lack cone function and have severely compromised rod function.[26] We found that these mice also performed at chance level (**Figure 5a**, 50.0 ± 6.2% correct choices, $N = 9$), and in addition, had significantly longer latency times to locate a platform (double knockout: 27.1 ± 4.0 seconds compared to wild type: 5.7 ± 0.4 seconds, and CNGA3$^{-/-}$: 9.4 ± 1.0 seconds, $P < 0.0001$, respectively; representative swim paths are shown in **Figure 5b**). This verifies that mice indeed use visual information to navigate to the platforms in our test paradigm.

© The American Society of Gene & Cell Therapy

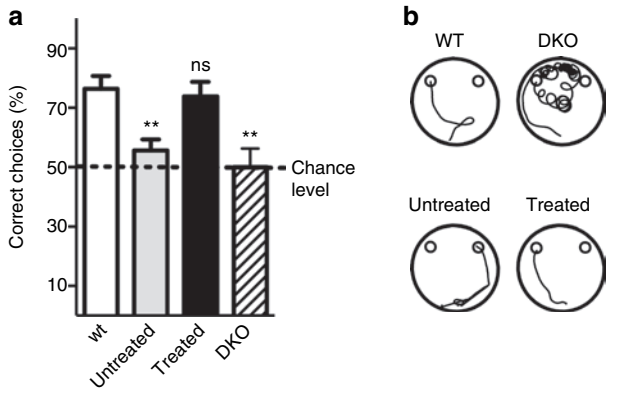

Figure 5 Gene replacement therapy enables cone-mediated visual processing in CNGA3$^{-/-}$ mice. (**a**) Treated mice display cone-mediated vision in a behavioral test. Mice were trained to associate a red-colored cue with a stable visible platform (acquisition). Subsequently, the mice had to discriminate between two visible platforms (discrimination), a stable platform (positioned next to the red cue = correct choice) and a platform that sank when a mouse climbed onto it (positioned next to a green cue = incorrect choice). The graph shows the mean percentage of correct choices for six trials during the discrimination test. The dotted line indicates the chance level. Statistical significance of differences from comparisons with wild type is shown on top of bars (**$P < 0.01$; ns, non-significant). (**b**) Representative swim paths of wild-type (wt), CNGA3/CNGB1 double knockout (DKO), untreated CNGA3$^{-/-}$ (untreated), and treated CNGA3$^{-/-}$ (treated) mice.

DISCUSSION

Cone vision is the most important visual quality in daytime environment. Inherited diseases such as achromatopsia lead to dysfunction and later degeneration of cone photoreceptors and are currently untreatable. With the advent of viral vectors capable of transducing retinal neurons, it seems feasible to develop gene therapies for inherited cone photoreceptor diseases. Here, we show that the principal subunit of the cone CNG channel (CNGA3) could successfully be produced in congenitally nonfunctional cone photoreceptors of CNGA3$^{-/-}$ mice. More importantly, this resulted in rescue of expression of the modulatory subunit of the cone CNG channel (CNGB3) and assembly of native cone CNG channel complexes that were correctly placed in the outer segments of cone photoreceptors. This is even more remarkable as there is evidence from previous studies that the ciliary transport from inner to outer segments is extremely sensitive and gets easily impaired in the diseased retina.[26–28]

The loss of CNGA3 profoundly impairs the Ca^{2+} homeostasis of cone photoreceptors, leading to a downregulation of key components of the visual transduction cascade.[7] In addition, we now provide, for the first time, experimental evidence for the presence of high, and potentially toxic cGMP levels in CNG channel–deficient cone photoreceptors. Importantly, our treatment strategy was able to reactivate the massively compromised signaling cascade and to lower the presumably detrimental[29] levels of cGMP, thereby restoring the light responsiveness of previously nonfunctional cones. The retinal ganglion cell recordings in combination with the behavioral data provide clear evidence that retinas with cones that are completely nonfunctional from birth can become capable of generating signals that higher visual centers can process in a way that permits the animal to successfully discriminate objects based on cone-mediated signals and take respective action. This result is a very promising and relevant aspect for future human use of this kind of therapeutic strategy.

Because mutations in CNG channel genes are the most common cause of human achromatopsia[2,30–32] (CNGB3 ≥50%, CNGA3 ≥25%, Gnat2 ≤2%), a large proportion of patients may benefit from such therapy. Although it will take some time until the results of long-term follow-up experiments are available, clues like the reduced activation of Müller cells and preserved number of cone photoreceptors suggest that the treatment also ameliorates the progressive cone degeneration.

In this study, we show that it is feasible to rescue fast degenerating (ventral) cone photoreceptors in CNGA3$^{-/-}$ mice at a time point when cone degeneration has already started.[7] One needs to consider that the situation in human achromatopsia patients may be different from that in CNGA3$^{-/-}$ mice. However, because cone degeneration in human achromats progresses very slowly[33–35] it may be possible to establish a treatment in adult patients.

MATERIALS AND METHODS

Animals. Animals were housed under standard white cyclic lighting (200 lux), had free access to food and water, and were used irrespective of gender. All procedures concerning animals were performed with permission of local authorities (Regierungspräsidium Tübingen and Regierung von Oberbayern) and in accordance with the ARVO Statement for the Use of Animals in Ophthalmic and Vision Research.

Cloning and production of rAAV vectors. Cloning and mutagenesis was performed by standard techniques. All sequence manipulations were confirmed by sequencing. To construct pAAV2.1-mBP-CNGA3, we inserted PCR amplified mouse CNGA3 complementary DNA (mA3F: 5′-GGATC TAGAGGATCCAGAGATGGCAAAGGTGAACACCCAG-3′ and mA3R: 5′-ATCCGGTCGACATCCCAGCACCCATGCTGGGT-3′, PCR template: mouse retinal complementary DNA) and a PCR amplified 0.5-kb mouse short wavelength opsin promoter fragment (mBPF: 5′-ATAGCTAGCA GGATGCAGTTGTTTCTG-3′, mBPR: 5′-GGACCGGTCCCGCTTGG GATGCCCTC-3′, PCR template: mouse genomic DNA) into pAAV2.1-mcs-WPRE, respectively. pAAV2.1-mcs was obtained by replacement of the CMV-eGFP sequence in pAAV2.1-CMV-eGFP (ref. 36) with a linker (5′-GGCCGCACCGGTACCTGGTAACCTCTAGAGTCGACA-3′). pAAV2/5Y719F encoding a Y719F-modified AAV5 capsid was obtained by site directed mutagenesis (YFF: 5′-CAGACCTATCGGAACCCGATTCC TTACCCGACCCCTTTAATTG-3′, YFR: 5′-CAATTAAAGGGGTCGGG TAAGGAATCGGGTTCCGATAGGTCTG-3′) using pAAV2/5 (ref. 37) as a template. Single-strand AAV vectors were produced by triple calcium phosphate transfection of 293T cells with pAdDeltaF6 (ref. 38), pAAV2/5Y719F, and pAAV2.1-mBP-CNGA3 plasmids followed by iodixanol-gradient[39] purification. The 40–60% iodixanol interface was further purified and concentrated by ion exchange chromatography on a 5 ml HiTrap Q Sepharose column using an ÄKTA Basic FPLC system (GE Healthcare, Munich, Germany) according to previously described procedures,[17] followed by further concentration using Amicon Ultra-4 Centrifugal Filter Units (Millipore, Schwalbach, Germany). Physical titers (in genome copies/ml) were determined by quantitative PCR of CNGA3 (A3qF: 5′-GAGCTACAATCAGAGCACCTGAC-3′ and A3qR: 5′-CCTTGCTCAAGGAAACCTGT-3′) using a LightCycler 480 (Roche Applied Science, Mannheim, Germany).

Subretinal rAAV injections. Mice were anesthetized by subcutaneous injection of ketamine (66.7 mg/kg) and xylazine (11.7 mg/kg), and their pupils were dilated with tropicamide eye drops (Mydriaticum Stulln; Pharma Stulln, Stulln, Germany). rAAV (1–1.5 µl) particles were injected into the

© The American Society of Gene & Cell Therapy

subretinal space using the NanoFil subretinal injection Kit (WPI, Berlin, Germany) equipped with a 34 gauge beveled needle. The injection was performed free hand under a surgical microscope (Carl Zeiss, Oberkochen, Germany). Special care was taken to avoid damage of the lens. The success of the procedure was monitored immediately following the injections using scanning laser ophthalmoscopy[18] and optical coherence tomography.[19] If the procedure was not successful (severe damage like a full retinal detachment), the mice were excluded from further analysis. At the given age, this concerned about one eye out of five.

ERGs. ERG analysis was performed 6, 10, and 11 weeks after injection according to procedures described elsewhere.[20,22] Single flash intensity and flicker frequency series data were available from 11 animals (one treated eye, one untreated eye). The 6 Hz flicker intensity series data were available from three animals (one treated eye, one untreated eye). Control data for **Figure 1** were obtained from four age-matched wild-type and 4-week-old rho$^{-/-}$ mice.[40]

Immunohistochemistry. Immunohistochemical staining was performed at ≥11 weeks after injection according to procedures described previously.[7] We used the following primary antibodies: rabbit anti-CNGA3 (refs. 6,7; 1:3,000), rabbit anti-CNGB3 (ref. 7; 1:2,000), rabbit anti-M-opsin[7] and anti-S-opsin[7] (1:300; Millipore), goat anti-S-opsin[41] (1:50; Santa Cruz Biotechnologies, Heidelberg, Germany), sheep anti-cGMP[23] (1:3,000), Cy3-coupled anti-glial fibrilary acid protein[7] (1:1,000; Sigma-Aldrich, Munich, Germany), and guinea-pig anti-glycogen phosphorylase (1:1,000).[42] For co-labeling with M-opsin, anti-CNGA3 was covalently labeled with DY-547 or DY-631-NHS esters (Dyomics, Jena, Germany). Fluorescein isothiocyanate–coupled peanut agglutinin (1:100; Sigma-Aldrich) was used as a cone marker (that labels inner and outer segments).[7] Laser scanning confocal micrographs were collected using an LSM 510 meta microscope (Carl Zeiss). Images shown in **Figures 2a–f** and **3b–g** represent collapsed confocal z-stacks. Stainings were reproduced in ≥3 independent experiments.

Ganglion cell recordings. Spike trains of retinal ganglion cells were recorded extracellularly with commercial planar multielectrode arrays (Multi Channel Systems, Reutlingen, Germany). Retinas of dark-adapted mice were isolated from the eye cup under infrared illumination, cut in half, and placed ganglion cell side down on an array of 60 electrodes with a minimum electrode spacing of 100 µm. In recordings from treated retinas, placement of the retina roughly aimed at covering the electrode array with the treated region of the retina. During recordings, the retina was continuously superfused with Ames medium, buffered with 22 mmol/l $NaHCO_3$ and 5% CO_2/95% O_2 (pH 7.4), and maintained at 35 °C. In each experiment, stable recording conditions of several hours were obtained. Voltage traces from the electrodes were amplified and stored digitally for offline analysis. Custom-made software was used for spike detection and spike clustering. Only units whose clusters were well separated and that showed a clear refractory period were used in the analysis. To visually stimulate the retina, the screen of a cathode ray tube monitor was focused with standard optics onto the photoreceptor layer, covering the recorded piece of retina. Periodic flashes were produced by switching the monitor display every 1 second between black and white, with a contrast (white − black)/(white + black) = 0.97. Overall light level was controlled with neutral density filters in the light path. Recordings for different light levels were always performed in the order of increasing intensities. For each light level, a 10–15 minute adaptation period at constant illumination preceded the recordings.

Two-choice cued water maze task. A modified version of the Morris water maze was used to test cone visual function. Mice were housed separately in a normal 12 hours light/dark cycle. The experiment was performed in the light cycle at photopic light conditions (111.0 ± 2.2 lux). On the day before the experiment, mice were habituated to the water (21 ± 1 °C, made opaque by the addition of nontoxic white dye) and to a stable platform in a 60 cm × 60 cm box. On the following day (day 1) mice were trained for six trials to associate a red cue (a rectangle attached to the maze wall next to the platform) with a stable visible platform (10 cm in diameter) that was placed in a circular swimming pool (120 cm in diameter, 70 cm high, white plastic) filled with water up to a depth of 30 cm. The reflectance of the red-colored cue was half-maximal at 590 nm (peak 660 nm). This is well within the spectral window of the wild-type mouse M-opsin (log relative sensitivity (−) 1.5 at 600 nm),[43–45] which suggests that this cue should be detected by the M cones of mice. The position of the platform was changed from trial to trial in a pseudorandom order to avoid association of the platform with distal spatial cues. On day 2, the animals had to discriminate between two visible platforms (10 cm in diameter, 10 cm distance from maze wall, 70 cm distance between the platforms). One platform was stable (marked with the red rectangle; correct choice) and the other platform sank when a mouse climbed onto it (marked with a green rectangle (reflectance: half-maximal 485 nm, peak 525 nm); incorrect choice). Trials were terminated if the mouse climbed on one of the two platforms. In case of wrong decisions, mice were placed on the "correct" platform, where all animals remained for 10 seconds before they were removed. After each trial, the mice were towel-dried, transferred to their home cage, and warmed using a heating lamp. Platforms were cleaned thoroughly between all trials to remove potential proximal cues (*e.g.*, urine). Visual performance was assessed during six trials separated by 60-minute intermissions. The number of correct choices (represented as the percentage of the total number of choices) was used for the evaluation of cone visual function. The experiment was performed and analyzed blindly to the animal genotype.

Statistics. All values are given as mean ± SE, and N is the number of animals. An unpaired Student's t-test was performed for the comparison between two groups. Values of $P < 0.05$ were considered significant.

SUPPLEMENTARY MATERIAL

Video S1. Example video showing the performance of a treated CNGA3$^{-/-}$ mouse on day 1 (training) in the cued water maze test.

Video S2. Example video showing the performance of a treated CNGA3$^{-/-}$ mouse on day 2 (test) in the cued water maze test.

ACKNOWLEDGMENTS

We thank Wolfgang Rödl for help with rAAV purification, Jennifer Schmidt, Gudrun Utz, and Stephanie Stark for excellent technical help, Tobias Gokus (University of Munich) for helpful discussion, Peter Humphries (Trinity College Dublin) for providing rho$^{-/-}$ mice, James M. Wilson (University of Pennsylvania) and Alberto Auricchio (TIGEM) for the gift of AAV plasmids, Jan de Vente (University og Maastricht) and Brigitte Pfeiffer-Guglielmi (University of Tübingen) for the gift of antibodies. This work was supported by the Deutsche Forschungsgemeinschaft (Se837/6-1, Se837/7-1, Pa1751/1-1, Bi484/4-1, and SFB 870), the German Ministry of Education and Research (BMBF 0314106), the European Union (EU HEALTH-F2-2008-200234), and the Max Planck Society.

REFERENCES

1. Peng, C, Rich, ED and Varnum, MD (2004). Subunit configuration of heteromeric cone cyclic nucleotide-gated channels. *Neuron* **42**: 401–410.
2. Kohl, S, Varsanyi, B, Antunes, GA, Baumann, B, Hoyng, CB, Jägle, H *et al.* (2005). CNGB3 mutations account for 50% of all cases with autosomal recessive achromatopsia. *Eur J Hum Genet* **13**: 302–308.
3. Deeb, SS (2005). The molecular basis of variation in human color vision. *Clin Genet* **67**: 369–377.
4. Jagla, WM, Jägle, H, Hayashi, T, Sharpe, LT and Deeb, SS (2002). The molecular basis of dichromatic color vision in males with multiple red and green visual pigment genes. *Hum Mol Genet* **11**: 23–32.
5. Kohl, S, Marx, T, Giddings, I, Jägle, H, Jacobson, SG, Apfelstedt-Sylla, E *et al.* (1998). Total colourblindness is caused by mutations in the gene encoding the α-subunit of the cone photoreceptor cGMP-gated cation channel. *Nat Genet* **19**: 257–259.
6. Biel, M, Seeliger, M, Pfeifer, A, Kohler, K, Gerstner, A, Ludwig, A *et al.* (1999). Selective loss of cone function in mice lacking the cyclic nucleotide-gated channel CNG3. *Proc Natl Acad Sci USA* **96**: 7553–7557.
7. Michalakis, S, Geiger, H, Haverkamp, S, Hofmann, F, Gerstner, A and Biel, M (2005). Impaired opsin targeting and cone photoreceptor migration in the retina of mice lacking the cyclic nucleotide-gated channel CNGA3. *Invest Ophthalmol Vis Sci* **46**: 1516–1524.

© The American Society of Gene & Cell Therapy

8. Acland, GM, Aguirre, GD, Ray, J, Zhang, Q, Aleman, TS, Cideciyan, AV *et al.* (2001). Gene therapy restores vision in a canine model of childhood blindness. *Nat Genet* **28**: 92–95.
9. Ali, RR, Sarra, GM, Stephens, C, Alwis, MD, Bainbridge, JW, Munro, PM *et al.* (2000). Restoration of photoreceptor ultrastructure and function in retinal degeneration slow mice by gene therapy. *Nat Genet* **25**: 306–310.
10. Bainbridge, JW, Smith, AJ, Barker, SS, Robbie, S, Henderson, R, Balaggan, K *et al.* (2008). Effect of gene therapy on visual function in Leber's congenital amaurosis. *N Engl J Med* **358**: 2231–2239.
11. Cideciyan, AV, Aleman, TS, Boye, SL, Schwartz, SB, Kaushal, S, Roman, AJ *et al.* (2008). Human gene therapy for RPE65 isomerase deficiency activates the retinoid cycle of vision but with slow rod kinetics. *Proc Natl Acad Sci USA* **105**: 15112–15117.
12. Hauswirth, WW, Aleman, TS, Kaushal, S, Cideciyan, AV, Schwartz, SB, Wang, L *et al.* (2008). Treatment of leber congenital amaurosis due to RPE65 mutations by ocular subretinal injection of adeno-associated virus gene vector: short-term results of a phase I trial. *Hum Gene Ther* **19**: 979–990.
13. Maguire, AM, Simonelli, F, Pierce, EA, Pugh, EN Jr, Mingozzi, F, Bennicelli, J *et al.* (2008). Safety and efficacy of gene transfer for Leber's congenital amaurosis. *N Engl J Med* **358**: 2240–2248.
14. Alexander, JJ, Umino, Y, Everhart, D, Chang, B, Min, SH, Li, Q *et al.* (2007). Restoration of cone vision in a mouse model of achromatopsia. *Nat Med* **13**: 685–687.
15. Chang, B, Dacey, MS, Hawes, NL, Hitchcock, PF, Milam, AH, Atmaca-Sonmez, P *et al.* (2006). Cone photoreceptor function loss-3, a novel mouse model of achromatopsia due to a mutation in Gnat2. *Invest Ophthalmol Vis Sci* **47**: 5017–5021.
16. Akimoto, M, Filippova, E, Gage, PJ, Zhu, X, Craft, CM and Swaroop, A (2004). Transgenic mice expressing Cre-recombinase specifically in M- or S-cone photoreceptors. *Invest Ophthalmol Vis Sci* **45**: 42–47.
17. Petrs-Silva, H, Dinculescu, A, Li, Q, Min, SH, Chiodo, V, Pang, JJ *et al.* (2009). High-efficiency transduction of the mouse retina by tyrosine-mutant AAV serotype vectors. *Mol Ther* **17**: 463–471.
18. Seeliger, MW, Beck, SC, Pereyra-Muñoz, N, Dangel, S, Tsai, JY, Luhmann, UF *et al.* (2005). *In vivo* confocal imaging of the retina in animal models using scanning laser ophthalmoscopy. *Vision Res* **45**: 3512–3519.
19. Fischer, MD, Huber, G, Beck, SC, Tanimoto, N, Muehlfriedel, R, Fahl, E *et al.* (2009). Noninvasive, *in vivo* assessment of mouse retinal structure using optical coherence tomography. *PLoS ONE* **4**: e7507.
20. Seeliger, MW, Grimm, C, Ståhlberg, F, Friedburg, C, Jaissle, G, Zrenner, E *et al.* (2001). New views on RPE65 deficiency: the rod system is the source of vision in a mouse model of Leber congenital amaurosis. *Nat Genet* **29**: 70–74.
21. Humphries, MM, Rancourt, D, Farrar, GJ, Kenna, P, Hazel, M, Bush, RA *et al.* (1997). Retinopathy induced in mice by targeted disruption of the rhodopsin gene. *Nat Genet* **15**: 216–219.
22. Tanimoto, N, Muehlfriedel, RL, Fischer, MD, Fahl, E, Humphries, P, Biel, M *et al.* (2009). Vision tests in the mouse: functional phenotyping with electroretinography. *Front Biosci* **14**: 2730–2737.
23. Tanaka, J, Markerink-van Ittersum, M, Steinbusch, HW and De Vente, J (1997). Nitric oxide-mediated cGMP synthesis in oligodendrocytes in the developing rat brain. *Glia* **19**: 286–297.
24. Baehr, W and Palczewski, K (2009). Focus on molecules: guanylate cyclase-activating proteins (GCAPs). *Exp Eye Res* **89**: 2–3.
25. Luo, DG, Xue, T and Yau, KW (2008). How vision begins: an odyssey. *Proc Natl Acad Sci USA* **105**: 9855–9862.
26. Hüttl, S, Michalakis, S, Seeliger, M, Luo, DG, Acar, N, Geiger, H *et al.* (2005). Impaired channel targeting and retinal degeneration in mice lacking the cyclic nucleotide-gated channel subunit CNGB1. *J Neurosci* **25**: 130–138.
27. Karan, S, Zhang, H, Li, S, Frederick, JM and Baehr, W (2008). A model for transport of membrane-associated phototransduction polypeptides in rod and cone photoreceptor inner segments. *Vision Res* **48**: 442–452.
28. Zhang, H, Fan, J, Li, S, Karan, S, Rohrer, B, Palczewski, K *et al.* (2008). Trafficking of membrane-associated proteins to cone photoreceptor outer segments requires the chromophore 11-cis-retinal. *J Neurosci* **28**: 4008–4014.
29. Paquet-Durand, F, Hauck, SM, van Veen, T, Ueffing, M and Ekström, P (2009). PKG activity causes photoreceptor cell death in two retinitis pigmentosa models. *J Neurochem* **108**: 796–810.
30. Ahuja, Y, Kohl, S and Traboulsi, EI (2008). CNGA3 mutations in two United Arab Emirates families with achromatopsia. *Mol Vis* **14**: 1293–1297.
31. Kohl, S, Baumann, B, Rosenberg, T, Kellner, U, Lorenz, B, Vadalà, M *et al.* (2002). Mutations in the cone photoreceptor G-protein α-subunit gene GNAT2 in patients with achromatopsia. *Am J Hum Genet* **71**: 422–425.
32. Thiadens, AA, Roosing, S, Collin, RW, van Moll-Ramirez, N, van Lith-Verhoeven, JJ, van Schooneveld, MJ *et al.* (2010). Comprehensive analysis of the achromatopsia genes CNGA3 and CNGB3 in progressive cone dystrophy. *Ophthalmology* **117**: 825–30.e1.
33. Eksandh, L, Kohl, S and Wissinger, B (2002). Clinical features of achromatopsia in Swedish patients with defined genotypes. *Ophthalmic Genet* **23**: 109–120.
34. Khan, NW, Wissinger, B, Kohl, S and Sieving, PA (2007). CNGB3 achromatopsia with progressive loss of residual cone function and impaired rod-mediated function. *Invest Ophthalmol Vis Sci* **48**: 3864–3871.
35. Thiadens, AA, Slingerland, NW, Roosing, S, van Schooneveld, MJ, van Lith-Verhoeven, JJ, van Moll-Ramirez, N *et al.* (2009). Genetic etiology and clinical consequences of complete and incomplete achromatopsia. *Ophthalmology* **116**: 1984–9.e1.
36. Allocca, M, Mussolino, C, Garcia-Hoyos, M, Sanges, D, Iodice, C, Petrillo, M *et al.* (2007). Novel adeno-associated virus serotypes efficiently transduce murine photoreceptors. *J Virol* **81**: 11372–11380.
37. Hildinger, M, Auricchio, A, Gao, G, Wang, L, Chirmule, N and Wilson, JM (2001). Hybrid vectors based on adeno-associated virus serotypes 2 and 5 for muscle-directed gene transfer. *J Virol* **75**: 6199–6203.
38. Auricchio, A, Hildinger, M, O'Connor, E, Gao, GP and Wilson, JM (2001). Isolation of highly infectious and pure adeno-associated virus type 2 vectors with a single-step gravity-flow column. *Hum Gene Ther* **12**: 71–76.
39. Grieger, JC, Choi, VW and Samulski, RJ (2006). Production and characterization of adeno-associated viral vectors. *Nat Protoc* **1**: 1412–1428.
40. Jaissle, GB, May, CA, Reinhard, J, Kohler, K, Fauser, S, Lütjen-Drecoll, E *et al.* (2001). Evaluation of the rhodopsin knockout mouse as a model of pure cone function. *Invest Ophthalmol Vis Sci* **42**: 506–513.
41. Haverkamp, S, Wässle, H, Duebel, J, Kuner, T, Augustine, GJ, Feng, G *et al.* (2005). The primordial, blue-cone color system of the mouse retina. *J Neurosci* **25**: 5438–5445.
42. Pfeiffer-Guglielmi, B, Fleckenstein, B, Jung, G and Hamprecht, B (2003). Immunocytochemical localization of glycogen phosphorylase isozymes in rat nervous tissues by using isozyme-specific antibodies. *J Neurochem* **85**: 73–81.
43. Jacobs, GH, Fenwick, JC, Calderone, JB and Deeb, SS (1999). Human cone pigment expressed in transgenic mice yields altered vision. *J Neurosci* **19**: 3258–3265.
44. Jacobs, GH, Williams, GA, Cahill, H and Nathans, J (2007). Emergence of novel color vision in mice engineered to express a human cone photopigment. *Science* **315**: 1723–1725.
45. Jacobs, GH, Williams, GA and Fenwick, JA (2004). Influence of cone pigment coexpression on spectral sensitivity and color vision in the mouse. *Vision Res* **44**: 1615–1622.